Permeation Through CO_2 Selective Glassy Polymeric Membranes in the Presence of Hydrogen Sulfide

Colin A. Scholes, Geoff W. Stevens, and Sandra E. Kentish
Dept. of Chemical and Biomolecular Engineering, Cooperative Research Centre for Greenhouse Gas Technologies (CO2CRC), The University of Melbourne, Victoria 3010, Australia

DOI 10.1002/aic.12610
Published online March 31, 2011 in Wiley Online Library (wileyonlinelibrary.com).

Minor components present in feed gas streams can have a significant influence on the separation performance of polymeric membranes. Hydrogen sulfide is present in many of the processes where CO_2 capture is possible and can therefore undergo competitive sorption with CO_2 for transport through the membrane, as well as influence the membrane morphology inducing plasticization. This study investigates the change in CO_2 permeability and CO_2/N_2 selectivity of two glassy polymeric membranes; polysulfone and 6FDA-TMPDA, when 500 ppm H_2S is present in the gas mixture. The outcomes of this study reveal that H_2S in trace amounts has a strong influence on the separation performance of both membranes. For both membranes, a plasticization partial pressure ~0.5–0.6 kPa H_2S is observed. H_2S competitive sorption is also observed and is modeled by competitive dual-sorption theory. Results suggest that mixed gas permeation influences the amount of each gas immobilized within the Langmuir voids in addition to the expected competitive sorption effects. © 2011 American Institute of Chemical Engineers *AIChE J,* 58: 967–973, 2012

Keywords: gas separation, polymeric membranes, carbon dioxide, hydrogen sulfide, competitive sorption

Introduction

Gas separation glassy polymeric membranes are an important technology for carbon dioxide capture,[1] having shown strong potential in the separation of CO_2 from natural gas,[2,3] syngas,[3] and biogas.[4] All of these applications have a high CO_2 partial pressure, the key driving force for membrane separation.[5] Often, other gases are present in trace quantities that can influence membrane performance. In particular, hydrogen sulfide is a common component in natural gas, which often requires "sweetening." In syngas, H_2S is generated from the reduction of sulfur compounds present in the feed material. In biogas, H_2S is a product of anaerobic respiration. Separation processes exist that can remove the majority of H_2S from these processes, however, H_2S will remain at ppm levels and will therefore permeate through a membrane in competition with CO_2, reducing its separation performance.[6] H_2S may also induce plasticization in glassy polymeric membranes, which alters the polymeric structure and weakens the mechanical strength of the membrane.[7,8] This is known to accelerate aging effects and lead to membrane failure. To date, the effects of trace H_2S on CO_2-selective membranes have not been studied, with the majority of the research focused on testing novel membranes for their potential as H_2S-selective membranes.[9–14] However, understanding the effects of minor components, particular H_2S, in feed gas on the separation performance is critical for implementation of gas separation membranes in industrial situations. Here, the effects of H_2S at low

Correspondence concerning this article should be addressed to S. E. Kentish at sandraek@unimelb.edu.au.

partial pressures in a CO_2-N_2 gas mixture are studied to quantify their influence on the performance of two glassy CO_2-selective gas separation membranes; polysulfone and a fluorinated polyimide, 6FDA-TMPDA. The gas mixture, CO_2-N_2 with ppm H_2S, simulates conditions that membranes would experience in industrial processes. Polysulfone is a commercially available proven CO_2-selective membrane, while 6FDA-TMPDA is one of a class of new polyimides that have improved performance over existing commercial CO_2-selective materials.[1]

Theory

The concentration of gas in polymeric membranes below the glass transition temperature can successfully be described by the dual-mode sorption model.[15] Gas molecules are assumed to sorb via two mechanisms; molecules absorbed directly into the polymer matrix (dissolution) and molecules adsorbed into micro-cavities within the polymeric matrix, a product of the glassy polymeric chains never obtaining thermodynamic equilibrium. Hence, the concentration of gas A within a glassy polymeric membrane is defined as:

$$C_A = C_{DA} + C_{HA} = k_{DA}f_A + \frac{C'_{HA}b_Af_A}{1 + b_Af_A} \tag{1}$$

where C_{DA} is the concentration in the Henry's law region, dependent on the Henry's law constant (k_{DA}) and fugacity (f_A), while C_{HA} is the concentration in the micro-cavity region modeled by a Langmuir isotherm, dependent on the maximum gas concentration (C'_{HA}), the Langmuir affinity constant (b_A), and the gas fugacity.

Koros[16] extended the dual-mode sorption theory for binary gas mixtures, to account for competitive sorption effects, guided by relations developed for gas sorption to catalysts. The total concentration of gas sorbed in the polymer, C, for a binary mixture of gas A and B is[16]:

$$C = k_{DA}f_A + k_{DB}f_B + \frac{C'_{HA}b_Af_A + C'_{HB}b_Bf_B}{1 + b_Af_A + b_Bf_B} \tag{2}$$

where all parameters have the same definition as above, with the subscript denoting whether they are a function of gas A or B. This assumes that the Henry's Law component of the sorption term behaves ideally. The concentration of gas A within the membrane is therefore[6]:

$$C_A = C_{DA} + C_{HA} = k_{DA}f_A + \frac{C'_{HA}b_Af_A}{1 + b_Af_A + b_Bf_B} \tag{3}$$

And the concentration of gas B within the membrane is:

$$C_B = C_{DB} + C_{HB} = k_{DB}f_B + \frac{C'_{HB}b_Bf_B}{1 + b_Af_A + b_Bf_B} \tag{4}$$

When three gas components or more are present, the concentration of gas A becomes:

$$C_A = C_{DA} + C_{HA} = k_{DA}f_A + \frac{C'_{HA}b_Af_A}{1 + b_Af_A + b_Bf_B + b_Cf_C + \ldots} \tag{5}$$

The concentration of both gas A and B is reduced compared to the single gas case (Eq. 1), and is heavily dependent on the relationship between the affinity constants (b_i) and fugacity (f_i) of all components.

Paul and Koros[17] have proposed a model based on partial immobilization of gas molecules in the micro-cavities of the polymer leading to differences in the diffusion coefficients of gas in both regions. Importantly, they base their model on Fickian diffusion coefficients, rather than thermodynamic diffusion coefficients which are used in the comparable model developed by Petropoulos.[18] The Fickian diffusion coefficient is related to the thermodynamic diffusion coefficient by:

$$D_A = D_{TA}\frac{C_A}{f_A}\left(\frac{\partial f_A}{\partial C_A}\right)_{T,p} \tag{6}$$

These authors assume that the total gas concentration can be divided into a mobile part with a concentration C_{mA}, while the remainder is totally immobilized. The mobile gas consists of all the gas in the Henry's Law region (C_{DA}) and a fraction F_A of gas associated with the Langmuir region (C_{HA})[17]:

$$C_{mA} = C_{DA} + F_AC_{HA} = k_{DA}f_A + \frac{F_AC'_{HA}b_Af_A}{1 + b_Af_A} \tag{7}$$

The overall mobile gas is assumed to diffuse with a Fickian diffusion coefficient equivalent to that in the Henry's Law region so that:

$$N_A = -D_{DA}\left(\frac{\partial C_{mA}}{\partial x}\right) \tag{8}$$

Paul and Koros also assume a linear decrease in gas concentration across the membrane, and therefore the steady state concentration profile across a membrane of length l is[19]:

$$C_{mA} = (C_{mA2} - C_{mA1})\left(1 - \frac{x}{l}\right) + C_{mA1} \tag{9}$$

where C_{mA2} and C_{mA1} are the upstream and downstream concentrations of the mobile phase. Hence, substituting Eqs. 7 and 9 into 8, the observed permeability of pure Gas A can be determined:

$$\begin{aligned} P_A \equiv \frac{N_Al}{(f_{A2} - f_{A1})} &= \frac{D_{DA}(C_{mA2} - C_{mA1})}{(f_{A2} - f_{A1})} \\ &= \frac{D_{DA}}{(f_{A2} - f_{A1})}\left[\left(k_{DA} + \frac{F_AC'_{HA}b_A}{1 + b_Af_{A2}}\right)f_{A2} \right. \\ &\qquad \left. - \left(k_{DA} + \frac{F_AC'_{HA}b_A}{1 + b_Af_{A1}}\right)f_{A1}\right] \end{aligned} \tag{10}$$

For a binary mixture, the concentration of the mobile component for a binary mixture is:

$$C_{mA} = k_{DA}f_A + \frac{F_AC'_{HA}b_Af_A}{1 + b_Af_A + b_Bf_B} \tag{11}$$

Hence, the observed permeability of gas A for a binary mixture can be determined by substituting Eqs. 9 and 11 into Eq. 8.

$$\begin{aligned} P_A = \frac{D_{DA}}{\left(f_{A2} - f_{A1}\right)}&\left[\left(k_{DA} + \frac{F_AC'_{HA}b_A}{1 + b_Af_{A2} + b_Bf_{B2}}\right)f_{A2} \right. \\ &\left. - \left(k_{DA} + \frac{F_AC'_{HA}b_A}{1 + b_Af_{A1} + b_Bf_{B1}}\right)f_{A1}\right] \end{aligned} \tag{12}$$

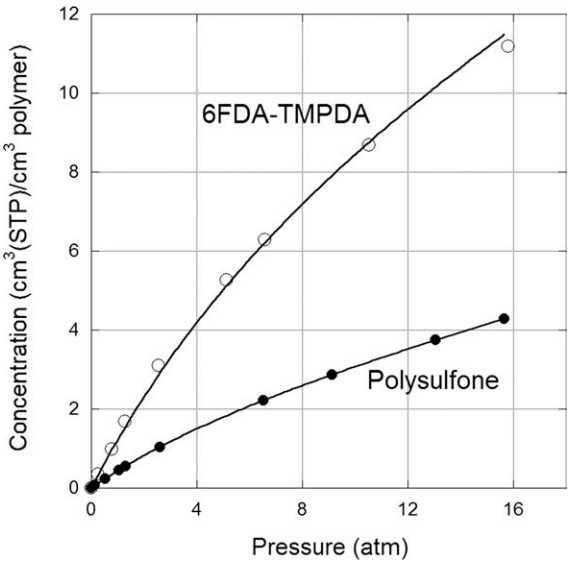

Figure 1. Concentration isotherms of N_2 in polysulfone and 6FDA-TMPDA at 35°C.

where f_{B2} and f_{B1} is the upstream and downstream fugacity of gas B respectively. Similarly, for a three component gas system the permeability of gas A can be determined:

$$P_A = \frac{D_{DA}}{(f_{A2} - f_{A1})}\left[\left(k_{DA} + \frac{F_A C'_{HA} b_A}{1 + b_A f_{A2} + b_B f_{B2} + b_C f_{C2}}\right) f_{A2} - \left(k_{DA} + \frac{F_A C'_{HA} b_A}{1 + b_A f_{A1} + b_B f_{B1} + b_C f_{C1}}\right) f_{A1}\right] \quad (13)$$

This multi-component competitive sorption permeability model does not have the same rigorous derivation as the comparable Petropoulos model,[15,18] and most specifically assumes that the mobile concentration of Species A falls linearly across the membrane film. This assumption may be less well justified in a multicomponent mixture, where the concentration of gas A also depends upon the concentration of other gas species. However, it provides a solution that allows the observed permeability to be modeled without detailed knowledge of the sorption behavior of the minor components. Specifically, only the Langmuir affinity parameters (b_B and b_C) for these species are required.

Experimental

The membranes studied were polysulfone (Aldrich) and 6FDA-TMPDA (2-2′-bis(3,4′-dicarboxyphenyl) hexafluoropropane dianhydrid-2,3,5,6-tetramethyl-1,4-phenylenediamine—synthesized in house[20]). All membranes were cast as flat dense sheets, from chloroform solvent for polysulfone and from dichloromethane solvent for 6FDA-TMPDA, following established procedures.[20] Membrane thicknesses were ~40 μm. Each membrane was dried at 100°C for 24 h under vacuum, and then annealed at 150°C for 48 h under vacuum. On completion of the annealing process, membranes were cooled slowly to room temperature under vacuum conditions, ~6 h and stored in a moisture free environment for less than a week, to minimize aging effects.

Sorption measurements were conducted on a Gravimetric Sorption Analyzer (GHP-FS, VTI Scientific Instruments, Florida), with a Cahn D-200 microbalance, as described elsewhere.[21] The membranes were initially exposed to vacuum overnight and heated to 120°C to remove air and water vapor. The penetrant gas was introduced into the chamber in pressure steps at 35°C and the equilibrium mass of membrane plus sorbed gas was measured. In an incremental manner, penetrant isotherms as a function of penetrant pressure were determined. Desorption isotherms were also measured and overlaid adsorption isotherm in all cases (i.e., no hysteresis was observed in the sorption-desorption behavior). Sorption mass equilibrium for all gases was reached within a maximum of 6 h at each pressure. A comparable experiment using helium was completed to determine the buoyancy correction.

The pure gas permeability through the membranes was undertaken on a constant volume, variable pressure gas permeation apparatus.[22] The apparatus operates by supplying feed gas at constant pressure to a preheating loop before proceeding to a sealed in house constructed membrane unit. The heating loop and membrane unit are housed in an oven for temperature control. The permeate gas passing into a cooling loop and known volume that is housed in a water bath, ensuring constant temperature of 25°C. Pressure increase in the permeate volume is determined by a MKS Baratron transducer, range 0–1.3 kPa absolute pressure. Before each gas permeability experiment, the total membrane system was evacuated, before the feed gas was applied, and the increase in pressure in the known permeate volume recorded every second. The permeability was then evaluated from Eq. 14; given the gas flux (Q) was determined from the pressure increase in the known volume, which thickness (l) and area (A) known:

$$P = \frac{Q \cdot l}{A \cdot \Delta P} \quad (14)$$

Mixed gas conditions were tested on different instrumentation, based on constant pressure[23] (Scholes et al., submitted). The membrane films were mounted on a porous stainless steel support in a 47 mm test cell, which was placed in an oven maintained at 15, 35 or 55°C. A feed stream of 90% N_2 – 10% CO_2 gas mixture (BOC Ltd., Australia) was passed across the retentate side of the membrane, while helium sweep gas (> 99%, BOC Australia) passed across the permeate side to prevent concentration polarization. The retentate pressure was varied, while the permeate side was at atmospheric pressure. Flow rates were maintained and monitored by digital mass flow controllers (Aalborg), with a back pressure regulator on the retentate side (Extech Technologies). Each membrane was exposed for 2 h until steady-state CO_2/N_2 separation had been obtained, then the feed gas was changed to 90% N_2 – 10% CO_2 with 500 ppm H_2S gas mixture (BOC Ltd Australia), with pressure and temperature conditions the same as before. The permeability of CO_2 and N_2 as well as selectivity were measured every 15 min until steady-state had been achieved, and the influence of H_2S observed. Concentrations of CO_2 and N_2 in the permeate gas were determined by gas chromatography (Varian CP-3800, column PORAPAK Q). It was not possible to detect H_2S due to the concentration being below the sensitivity of the gas chromatograph detector.

Modeling of the measured permeability of CO_2 under mixed gas conditions, with N_2 and H_2S present, was

Table 1. Dual-mode Sorption Parameters of CO_2 and N_2, k_D (cm^3(STP)/cm^3 atm), C'_H (cm^3(STP)/cm^3), b (atm^{-1}) and the Immobilization Factor (F) of CO_2 for Polysulfone and 6FDA-TMPDA at 35°C

	Polysulfone		6FDA-TMPDA	
	CO_2	N_2	CO_2	N_2
k_D (cm^3(STP)/cm^3 atm)	0.41	0.16	3.2	0.3
C'_H (cm^3(STP)/cm^3)	16.2	2.81	58.8	12.0
b (atm^{-1})	0.38	0.11	0.55	0.083
F	0.48	–	0.57	–

Carbon dioxide parameters are taken from Duthie *et al.* [22] and Scholes *et al.*[24]

undertaken using Eqs. 12 and 13. These equations require only the Langmuir affinity constant, b, for N_2 and H_2S. Conversely for CO_2, diffusivity and all other dual-mode sorption parameters are required.

Results and Discussion

Concentration isotherms of pure gases

The concentration isotherms of carbon dioxide in 6FDA-TMPDA[22] and polysulfone[24] have already been reported. The concentration isotherms of nitrogen in these materials are shown in Figure 1. These isotherms all demonstrate standard dual-sorption behavior as indicated by a rapid increase in gas concentration at low pressures, which tapers off at higher pressures to an almost linear relationship.[15] At low pressures, the microvoid space within the polymeric matrix is filled. As the pressure of the gas increases, the free microvoid space becomes limited and the concentration build-up is reduced to the sorption of gas in the polymeric matrix only. This follows Henry's law, hence the almost linear relationship at high pressures. The dual-mode sorption parameters for nitrogen in the two polymers were determined by fitting Eq. 1 to each isotherm, with the goodness of fit shown in Figure 1. The dual-sorption parameters for both gases are presented in Table 1. Also included in Table 1 are the immobilization factors for CO_2 at 35°C, as previously reported.[22,24]

The polysulfone dual-sorption values correspond well with those reported by Aitken et al.,[25] while the 6FDA-TMPDA N_2 values are similar to those reported for similar polyimides.[26,27] Shao et al.[28] has also reported dual-sorption parameters for CO_2 and N_2 in 6FDA-TMPDA. The values for CO_2 are similar to those used here, with small differences attributed to Shao et al.[28] only measuring CO_2 sorption to 8 atm, in comparison to 16 atm for the values used here. There is greater discrepancy between the dual sorption values for N_2, in particular the C'_H used here is half the value reported by Shao et al. and the b is almost double the value reported by Shao et al. These differences can be attributed to several possible causes; differences in membrane morphology because of different annealing history; inaccuracy in the sorption measurement because of the low solubility of N_2; and the interdependency of the two dual sorption parameters in the regression analysis.

CO_2 permeability under mixed gas conditions with N_2 and 500 ppm H_2S

The variation in CO_2 permeability through polysulfone and 6FDA-TMPDA after exposure to other gases in the feed at various total pressures can be seen in Figures 2 and 3.

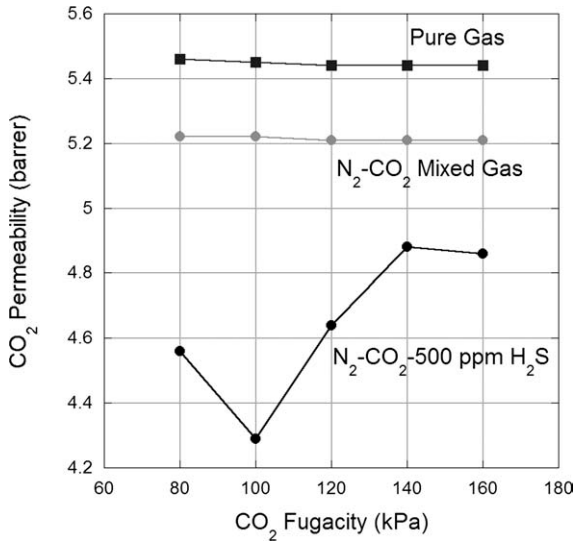

Figure 2. CO_2 permeability in polysulfone as a function of CO_2 fugacity for pure gas, N_2-CO_2 mixed gas conditions and N_2-CO_2 mixed gas with 500 ppm H_2S present, at 35°C.

Changes in CO_2 fugacity where achieved by changing the total feed pressure between 400–1600 kPa, so that both N_2 and H_2S fugacity also increase along this axis.

These graphs have been plotted with CO_2 fugacity on the x-axis, but it should be kept in mind that changes in CO_2 fugacity where achieved by changing the total feed pressure between 400 and 1600 kPa, so that both N_2 and H_2S fugacity also increase along this axis.

The permeability for pure CO_2 varies little with fugacity due to the relatively narrow range of fugacities studied.

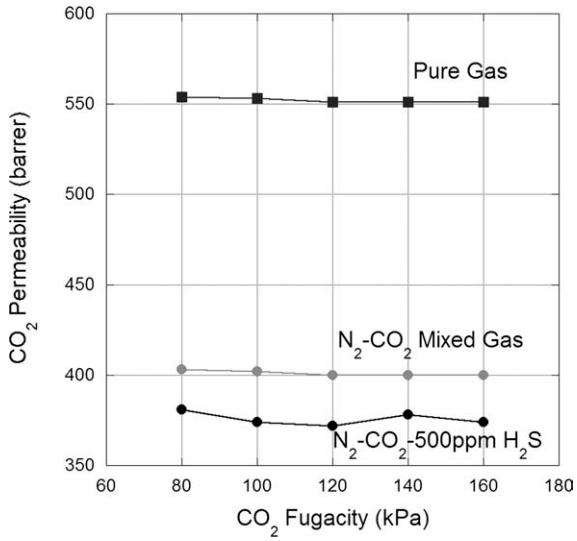

Figure 3. CO_2 permeability in 6FDA-TMPDA as a function of CO_2 fugacity for pure gas, N_2-CO_2 mixed gas conditions and N_2-CO_2 mixed gas with 500 ppm H_2S present, at 35°C.

Changes in CO_2 fugacity where achieved by changing the total feed pressure between 400–1600 kPa, so that both N_2 and H_2S fugacity also increase along this axis.

Table 2. CO_2 and N_2 Permeability through Polymeric Membranes under Pure Gas Conditions, 400 kPa at 35°C, compared with Literature Reported Values

	Polysulfone	6FDA-TMPA
CO_2 Permeability (barrer)	5.44	551
CO_2 Literature (barrer)	5.6[29]	577[22]
N_2 Permeability (barrer)	0.32	56.4

Literature data for CO_2 in polysulfone was recorded at a pressure of 20 atm,[29] while that for 6FDA-TMPDA was at 1000 kPa.[22]

These are all less than that required to plasticize each polymer; the plasticization pressure for polysulfone is 34 bar CO_2 at 21°C,[29] and 6FDA-TMPDA is plasticized by CO_2 at 14 bar at 35°C.[22] The permeability of CO_2 for the N_2-CO_2 feed mixture, with no H_2S present, are lower than those obtained for CO_2 under pure gas conditions (Table 2). This is a common observation for mixed gas systems,[30] due to competition with N_2 sorption within the membrane structure.

Upon exposure to H_2S, a reduction in the permeability of CO_2 occurs for both glassy membranes, at every partial pressure. This is due to competitive sorption between H_2S and CO_2 within the microvoids, where H_2S will replace some adsorbed CO_2, and reduce the concentration of CO_2 within the membrane. Clearly, H_2S strongly competes with CO_2 for space within these microvoids, given that H_2S has such a great impact when it is present only at ppm levels. Increasing the partial pressure of H_2S generally reduces the CO_2 permeability because the higher fugacity of the gas leads to stronger competitive sorption. However, increasing the H_2S partial pressure for polysulfone above 0.5 kPa (by increasing the total feed pressure to a corresponding CO_2 fugacity of above 100 kPa) results in a notable rise in CO_2 permeability, compared to the lower H_2S partial pressure measurements. This increase can not readily be accounted for by CO_2 plasticization, given that the membranes had been exposed to N_2-CO_2 gas mixture two hours prior to being exposed to 500 ppm H_2S. Rather, this is suggestive of partial plasticization of the membrane materials by H_2S, which increases the diffusivity of gases through the membrane due to disruption to the polymer chain—chain intermolecular bonding network.[8] This increases the fractional free volume and produces an increase in the measured permeability of gases.

Similar trends in the data were observed at 15°C and 55°C (data not shown) with evidence of H_2S plasticization also evident above a partial pressure of 0.5–0.6 kPa in the data for 6FDA-TMPDA at 15°C, where solubilities are higher than in the data presented here.

N_2 permeability under mixed gas conditions with N_2 and 500 ppm H_2S

N_2 also experiences competitive sorption from H_2S, and so the permeability of N_2 through both glassy polymeric membranes also decreases (Figures 4 and 5). The reduction is not as pronounced as observed for CO_2. H_2S undergoes stronger competitive sorption with CO_2, because a significant amount of the sorption of this gas occurs within the microvoids of the membrane, where N_2 sorption is low. Importantly, there is again some evidence of membrane plasticization at comparable partial pressures of H_2S, by the observed increase in N_2 permeability.

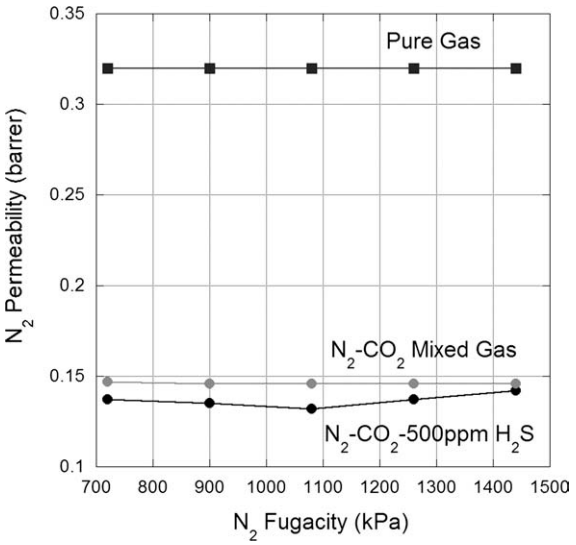

Figure 4. N_2 permeability in polysulfone as a function of N_2 fugacity for pure gas, N_2-CO_2 mixed gas conditions and N_2-CO_2 mixed gas with 500 ppm H_2S present, at 35°C.

Changes in N_2 fugacity where achieved by changing the total feed pressure between 400–1600 kPa, so that both CO_2 and H_2S fugacity also increase along this axis.

CO_2/N_2 selectivity under mixed gas conditions

For pure gas measurements, the CO_2/N_2 selectivity at 35°C is 17 for polysulfone and 9.8 for 6FDA-TMPDA. Under the N_2-CO_2 mixed gas conditions, CO_2/N_2 selectivity increases to 37 for polysulfone and 24 for 6FDA-TMPDA. This significant increase in ideal selectivity is the result of

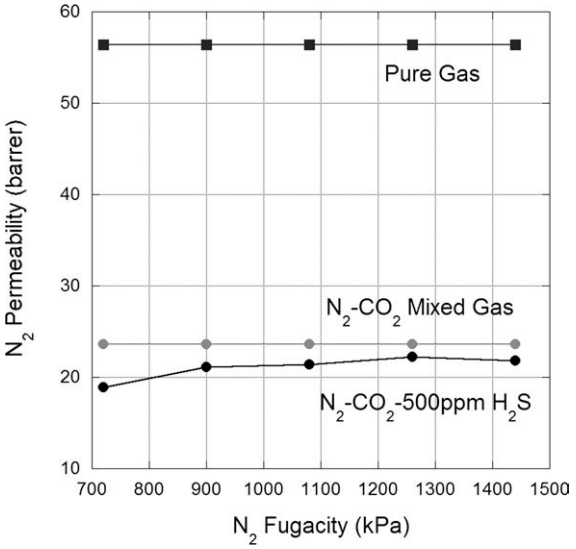

Figure 5. N_2 permeability in 6FDA-TMPDA as a function of N_2 fugacity for pure gas, N_2-CO_2 mixed gas conditions and N_2-CO_2 mixed gas with 500 ppm H_2S present, at 35°C.

Changes in N_2 fugacity where achieved by changing the total feed pressure between 400–1600 kPa, so that both CO_2 and H_2S fugacity also increase along this axis.

N_2 permeability experiencing a stronger competitive sorption effect from CO_2, compared with CO_2 permeability from N_2. For example, in 6FDA-TMPDA, CO_2 mixed gas permeability is reduced 27% compared with the pure gas case, while N_2 mixed gas permeability is reduced by 57% compared with the pure gas case (Figures 3 and 5). Hence, under mixed gas conditions the ideal selectivity of CO_2/N_2 increases.

With the addition of H_2S, the CO_2/N_2 selectivity for polysulfone reduces to an average of 35, while for 6FDA-TMPDA the selectivity reduces to an average of 21 across the pressure ranges studied. Hence, with the addition of H_2S, the permeability of CO_2 is reduced significantly from the pure gas case for both membranes, but the observed CO_2/N_2 selectivity reduction is less dramatic. Therefore, both membranes clearly retain the ability to achieve good CO_2 separation from N_2 in the presence of H_2S.

Competitive sorption modeling of CO_2 permeability under mixed gas conditions

To model the change in CO_2 permeability of both membranes from the pure gas to mixed gas systems, the following parameters need to be known: the Fickian diffusion coefficient (D_{DA}), Henry's Law constant (k_{DA}), maximum Langmuir capacity(C'_{HA}), and immobilization factor (F_A) for carbon dioxide; and the Langmuir coefficient (b) for all gases (CO_2, N_2, and H_2S).

We initially assumed that the Henry's Law constant (k_{DCO2}), maximum Langmuir capacity (C'_{HCO2}), Langmuir Coefficient (b_{CO2}) and the immobilization factor (F_{CO2}) for CO_2 were all equal to the pure gas case. The Langmuir Coefficient for N_2 (b_{N2}) was also taken from the pure gas case (Table 1). For 6FDA-TMPDA, values of the Fickian diffusion coefficient (D_{DCO2}) have been published as a function of CO_2 fugacity and these values were used directly.[22] For polysulfone, we took a more approximate approach, assuming that the average Fickian value can be approximated by the average thermodynamic value, which is determined from the pure gas permeability by:

$$\bar{D}_{DTCO2} \approx P_A \frac{(f_1 - f_2)}{(C_1 - C_2)} \tag{15}$$

Initially, these parameters were incorporated into Eq. 12, and this equation was fitted to the experimental data for the binary N_2-CO_2 system at 35°C. However, it was not possible to obtain a good fit to the data, with results over-predicting the CO_2 permeability. Specifically while our experimental results showed a mixed gas permeability of 5.2 Barrer in polysulfone and 400 Barrer in 6FDA-TMPDA, Eq. 12 gave values of 8.0 and 564 Barrer, respectively. This over prediction is believed to be associated with the diffusivity component of permeability rather than the solubility component, given that there is a well established theory for mixed gas sorption in polymeric films.[16] The most significant source of uncertainty in the diffusivity term is the immobilization factor, F_{CO2}, which accounts for the fraction of CO_2 immobilized within the microvoids. Under mixed gas conditions, the presence of N_2 and H_2S may influence the degree of immobilization by blocking diffusional pathways between micro-cavities. This will not influence the diffusivity through the Henry's law region of the polymer but will influence diffusivity through the micro-cavities, leading to an overall lower value for measured permeability. Hence to determine the change in immobilization factor under mixed gas conditions, a least squares minimization was used on Eqs. 12 and 13 relative to the experimental data.

Table 3. F_{CO2} under Mixed Gas Conditions for Polysulfone and 6FDA-TMPDA at 35°C

	CO_2-N_2	CO_2-N_2-H_2S
Polysulfone	0.25 ± 0.01	0.22 ± 0.01
6FDA-TMPDA	0.34 ± 0.01	0.33 ± 0.01

The resulting CO_2 immobilization factors under N_2-CO_2 mixed gas conditions for both membranes are provided in Table 3. For polysulfone, F_{CO2} is reduced by almost 50% in the mixed gas case compared with the pure gas case, while for 6FDA-TMPDA a 40% reduction is observed. This indicates that the fraction of CO_2 immobilized in the microvoids has increased as a result of N_2 being present. This result is interpreted by assuming that the large concentrations of N_2 partially occupy the pathways between microvoids, restricting CO_2 transport through the membrane.

To evaluate the tertiary system CO_2-N_2-H_2S, an estimate of the Langmuir affinity for hydrogen sulfide (b_{H2S}) is required. To the best of the authors' knowledge, there are no reported values of this parameter for polymeric membranes in the literature. Thus, we initially attempted a multivariate regression analysis to determine both b_{H2S} and F_{CO2} from the experimental data. However, this created too many degrees of freedom in the regression analysis, leading to large error margins around both parameters. As an alternative, we estimated the b_{H2S} value from reported concentration isotherms of H_2S in ethylcellulose and cellulose acetate.[9] Fitting the dual-sorption model (Eq. 1) to these isotherms gives a value of b_{H2S} for ethylcelluose of 24 (−35°C) and 8.7 (0°C) and for cellulose acetate a value of 16.5 atm^{-1} (0°C). Further, it has been shown that there is a correlation between the Langmuir affinity of a gas for any polymeric membrane and its critical temperature,[30] a measure of a molecule's condensability. Higher critical temperature corresponds to a greater affinity constant. This correlation suggests values for b_{H2S} between 5 and 25 atm^{-1} at 35°C (T_C 373.2 K[30]). In the present case, we assume a value of $b_{H2S} = 15 \pm 10$ atm^{-1}.

These parameters were incorporated into Eq. 13 and this equation was fitted to the experimental data using a least squares minimization approach, with the variable the immobilization factor, F_{CO2}, and the initial value that determined for the N_2-CO_2 gas mixture system (Table 3). To eliminate the effect of plasticization at high H_2S partial pressures, data analysis was restricted to partial pressures below 0.6 kPa H_2S. The resulting immobilization factors under mixed gas conditions with H_2S present are provided in Table 3. For 6FDA-TMPDA, F_{CO2} is only slightly reduced by 3% compared to the CO_2-N_2 system, which is within the error of the measurement. This implies that no change in the immobilization factor is required to account for H_2S competitive sorption. Therefore, these low concentrations of H_2S have little influence on CO_2 diffusion through 6FDA-TMPDA. For polysulfone, a reduction of 12% is observed, indicating a slight

decrease in the diffusion rate of CO_2 through the microvoid region in this case. The difference between the two polymers is attributed to the different morphology, with 6FDA-TMPDA having a greater fractional free volume compared with polysulfone, as indicated by the larger maximum Langmuir coefficient.

Conclusion

Polysulfone and 6FDA-TMPDA membranes have reduced CO_2 separation performance due to the presence of trace amounts of H_2S in the feed gas, for all pressures and temperatures studied. The loss of both permeability and selectivity arises from competitive sorption of H_2S within the microvoids. At higher pressures and lower temperatures, H_2S also appears to induce plasticization, further altering the separation performance. Modeling of the multi-gas competitive sorption system indicated that the loss in performance could not be accounted for simply through the introduction of additional Langmuir sorption. Rather, competitive sorption appeared to also lead to further immobilization of carbon dioxide within the microvoids. Hence, future research is required to independently evaluate the immobilization factor for individual gases in multi-gas membrane systems.

Acknowledgments

The authors thank the Particulate Fluids Processing Centre, a Special Research Centre of the Australian Research Council for access to equipment. The authors also acknowledge the funding provided by the Australian Government through its CRC Program to support this CO2CRC research project.

Literature Cited

1. Powell CE, Qiao GG. Polymeric CO2/N2 gas separation membranes for the capture of carbon dioxide from power plant flue gases. *J Membr Sci*. 2006;279:1–49.
2. Stern SA. Polymers for gas separations: the next decade. *J. Membr Sci*. 1994;94:1–65.
3. Metz B, Davidson O, de Coninck H, Loos M, Meyer L, editors. *IPCC Special Report on Carbon Dioxide Capture and Storage*, Cambridge, UK: Cambridge University Press, 2005.
4. Harasimowicz M, Orluk P, Zakrzewska-Trznadel G, Chmielewski AG. Application of polyimide membranes for biogas purification and enrichment. *J Hazardous Mat*. 2007;144:698–702.
5. Paul D, Yampol'skii Y. *Polymeric gas separation membranes*. Baton Rouge: CRC Press, 1994.
6. Koros WJ, Chern RT, Stannett V, Hopfenberg HB. A model for permeation of mixed gases and vapors in glassy polymers. *J Polym Sci Polym Phys Ed*. 1981;19:1513–1530.
7. Kesting RE, Fritzche AK. *Polymeric Gas Separation Membranes*. New York: Wiley, 1993.
8. Stern SA, Saxena V. Concentration dependent transport of gases and vapors in glassy polymers. *J Membr Sci*. 1980;7:47–59.
9. Heilman W, Tammela V, Meyer JA, Stannett V, Szwarc M. Permeability of polymer films to hydrogen sulfide gas. *Ind Eng Chem*. 1956;48:821–824.
10. Orme CJ, Stewart FF. Mixed gas hydrogen sulfide permeability and separation using supported polyphosphazene membranes. *J Membr Sci*. 2005;253:243–249.
11. Merkel TC, Toy LG. Comparison of hydrogen sulfide transport properties in fluorinated and nonfluorinated polymers. *Macromolecules*. 2006;39:7591–7600.
12. Hao J, Rice PA, Stern SA. Upgrading low-quality natural gas with H2S- and CO2-selective polymer membranes. Part I. Process design and economics of membrane stages without recycle streams. *J Membr Sci*. 2002;209:177–206.
13. Heyd RL, McCandless FP. Separation of H2S from N2 by selective permeation through polymeric membranes. *J Membr Sci*. 1977;2:375–389.
14. Chatterjee G, Houde AA, Stern SA. Poly(ether urethane) and poly (ether urethane urea) membranes with high H2S/CH4 selectivity. *J Membr Sci*. 1997;135:99–106.
15. Petropoulos JH. *Mechanisms and theories for sorption and diffusion of gases in polymers*. In: Paul DR, Yampol'skii Y, editors. *Polymeric Gas Separation Membranes*. Boca Raton, FL: CRC Press 1994:17–81.
16. Koros WJ. Model for sorption of mixed gases in glassy polymers. *J Polym Sci Polym Phys Ed*. 1980;18:981–992.
17. Paul DR, Koros WJ. Effect of partially immobilizing sorption on permeability and the diffusion time lag. *J Polym Sci Polym Phys*. 1976;14:675–685.
18. Petropoulos JH. Quantitative analysis of gaseous diffusion in glassy polymers. *J Polym Sci Polym Phys*. 1970;1797–1801.
19. Paul DR. Effect of immobilizing adsorption on the diffusion time lag. *J Polym Sci A-2*. 1969;7:1811–1818.
20. Powell CE, Duthie XJ, Kentish SE, Qiao GG, Stevens GW. Reversible Diamine cross-linking of polyimide membranes. *J Membr Sci*. 2007;291:199–209.
21. Scholes CA, Tao WX, Kentish SE, Stevens GW. Sorption of gases and water in Matrimid 5218. *J Appl Polym Sci*. 2010;117:2284–2289.
22. Duthie XJ, Kentish SE, Powell CE, Nagai K, Qiao GG, Stevens GW. Operating temperature effects on the plasticization of polyimide gas separation membranes. *J Membr Sci*. 2007;294:40–49.
23. Anderson CJ, Pas SJ, Arora G, Kentish SE, Hill AJ, Sandler SI, Stevens GW. Effect of pyrolysis temperature and operating temperature on the performance of nanoporous carbon membranes. *J Membr Sci*. 2008;322:19–27.
24. Scholes CA, Kentish SE, Stevens GW. Plasticization of asymmetric polysulfone membranes by carbon dioxide. *J Membr Sci*. 2010;346: 208–214.
25. Aitken CL, Koros WJ, Paul DR. Gas transport properties of biphenol polysulfones. *Macromolecules*. 1992;25:3651–3658.
26. Chung TS, Cao C, Wang R. Pressure and temperature dependence of the gas-transport properties of dense poly(2,6-toluene-2,2-bis(3,4-dicarboxylphenyl) hexafluoropropane diimide) membranes. *J Polym Sci B*. 2004;42:354–364.
27. Wang R, Chan SS, Liu SL, Chung TS. Gas transport properties of poly(1,5-naphthalene-2,2′-bis(3,4-phthalic) hexafluoropropane) diimide (6FDA-,1,5-NDA) dense membranes. *J Membr Sci*. 2002;199: 191–202.
28. Shao L, Chung TS, Pramoda KP. The effects of 1,3-cyclohexane-bis(methylamine) modification on gas transport and plasticization resistance of polyimide membranes. *J Membr Sci*. 2005;267:78–89.
29. Aitken CL, Koros WJ, Paul DR. Effect of structural symmetry on gas transport properties of polysulfones. *Macromolecules*. 1992;25: 3424–3434.
30. Scholes CA, Kentish SE, Stevens GW. Effects of minor components in carbon dioxide capture using polymeric gas separation membranes. *Sep Purif Rev*. 2009;38:1–44.

Manuscript received Sep. 28, 2010, and revision received Feb. 18, 2011.